ACS OMEGA

Article

http://pubs.acs.org/journal/acsodf

Role of Molecular Polarity in Thermal Transport of Boron Nitride−Organic Molecule Composites

Ruimin Ma,[†,‡,∥] Xiao Wan,[†,§,∥] Teng Zhang,[‡] Nuo Yang,*[,†,§] and Tengfei Luo*[,‡]

[†]State Key Laboratory of Coal Combustion and [§]Nano Interface Center for Energy, School of Energy and Power Engineering, Huazhong University of Science and Technology, Wuhan 430074, China

[‡]Department of Aerospace and Mechanical Engineering, University of Notre Dame, Notre Dame, Indiana 46556, United States

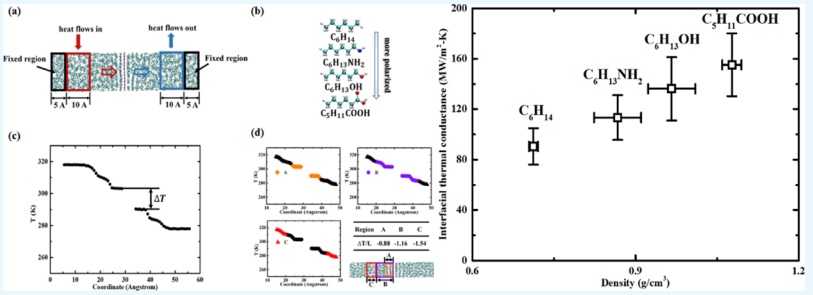

ABSTRACT: Understanding the role of fillers in the thermal transport of composite materials is of great importance to engineering better materials. The filler induces material interfaces within the composite, which influence the thermal transport between the matrix and themselves. The filler can also alter the molecular arrangement of the matrix in its vicinity, which may also impact the thermal transport ability. In this paper, molecular dynamics simulations are performed to study the thermal transport across the matrix−filler interfaces in hexagonal boron nitride (h-BN)−organic molecule composites. Four different organic molecules are studied as the matrixes. They include hexane (C_6H_{14}), hexanamine ($C_6H_{13}NH_2$), hexanol ($C_6H_{13}OH$), and hexanoic acid ($C_5H_{11}COOH$), which feature the same molecular backbone but increasingly different polar functional groups. The nominal local thermal conductivities of the hexane matrix with varying distances to the interface are calculated to demonstrate the influence of the filler on the thermal transport properties of the matrix. It is found that a more polar matrix exhibits a higher density in the near-interface region and a higher nominal local thermal conductivity, suggesting that the interfacial interaction can impact the local heat transfer ability of the matrix. In addition, the more polar matrix also leads to a larger interfacial thermal conductance with h-BN (hexane: 90.47 ± 14.49 MW/m^2 K, hexanamine: 113.38 ± 17.72 MW/m^2 K, hexanol: 136.16 ± 25.12 MW/m^2 K, and hexanoic acid: 155.17 ± 24.89 MW/m^2 K) because of the higher matrix density near the interface and thus more atoms exchanging energy with the filler. The results of this study may provide useful information for designing composite materials for heat transfer applications.

INTRODUCTION

Thermal transport is critical to a wide range of applications such as advanced electronics,[1,2] optoelectronics, photovoltaic solar cells,[3] and Li-ion batteries.[4] It is also the key to determining the lifetime and performance of these devices. There has been an increasing demand for polymeric materials with high thermal conductivity that can dissipate heat generated by electronic devices in operation. To create efficient heat transfer pathways, various attempts have been exploited to increase the thermal conductivity of these materials by compositing high thermal conductivity fillers, such as carbonaceous materials, boron nitride, and silicon nitride.[5−15] Thus, to facilitate the design of nanocomposites with high thermal conductivity, a fundamental and comprehensive understanding of the thermal transport in polymeric nanocomposites is essential.

Though it is universally known that adding high thermal conductivity materials into a low thermal conductivity matrix can improve the thermal transport,[16,17] the fundamental mechanism that links the role of fillers to the overall thermal transport in nanocomposites is still lacking. A typical problem being addressed in nanocomposites is the thermal transport across the interface between the matrix and the fillers.[18,19] Extensive studies have demonstrated that the interface plays a critical role in determining the thermal energy transport in nanocomposites, as the interface can influence and even dominate the thermal transport in nanocomposites.[16,17] Recent studies show that the interfacial thermal resistance could be decreased by tuning the alignment or surface functionalization of graphene in composites.[18,20] Most of these studies only address the heat flux exchange across the interface. Beyond the direct impact on interfacial thermal conductance, the fillers also affect the nominal local thermal conductivity of the matrix, which has been studied much less intensively. It has been

Received: September 10, 2018
Accepted: September 24, 2018

DOI: 10.1021/acsomega.8b02338
ACS Omega XXXX, XXX, XXX−XXX

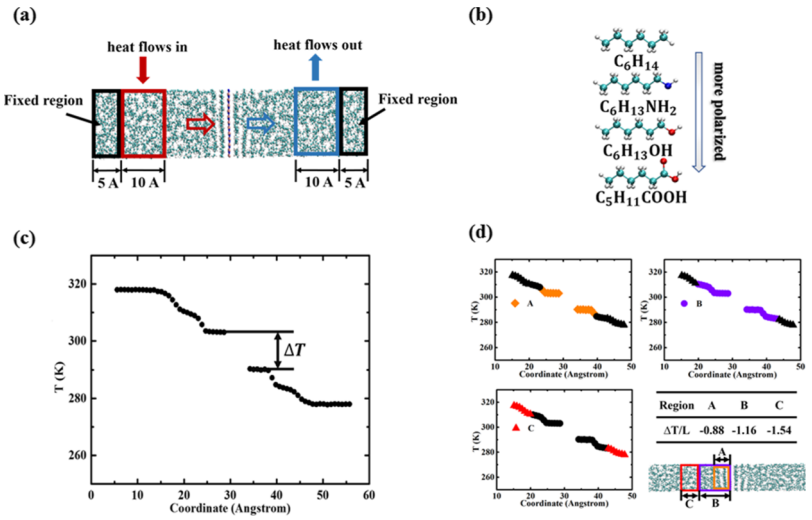

Figure 1. (a) Simulation setup for ITC calculations in the NEMD method: heat flows across the interface from the heat source (red region) to the heat sink (blue region), with the fixed regions (black region) set at the end of the system; the arrows in the graph represent the direction of heat flow; the length of both the heat source and heat sink is 10 Å, and the length of each fixed region is 5 Å. (b) The chemical structures of hexane (C_6H_{14}), hexanamine ($C_6H_{13}NH_2$), hexanol ($C_6H_{13}OH$), and hexanoic acid ($C_5H_{11}COOH$); the order of polarity is $C_5H_{11}COOH$ > $C_6H_{13}OH$ > $C_6H_{13}NH_2$ > C_6H_{14}. (c) Steady-state temperature profile of the simulation system (shown in a) and the temperature difference (ΔT) across the interface. (d) Temperature points leveraged to calculate ΔT for regions A, B, and C (highlighted in different colors), where ΔT is the temperature difference between the two ends of the chosen region and $\Delta T/L$ is the temperature difference divided by the region length in each region; the smaller the absolute value of $\Delta T/L$, the larger the nominal local thermal conductivity.

demonstrated that the arrangement of matrix molecules close to the interface is influenced by their dipoles,[21,22] resulting in a different density near the interface.[23,24] This may imply that the nominal local thermal properties of the matrix can also be changed by the fillers, as the thermal conductivity of polymers is a strong function of their molecular-level conformations.[25,26]

In this work, we perform molecular dynamics (MD) simulations and analyses to explore the impact of the h-BN fillers on the thermal transport. As an insulator, h-BN fillers are preferred over graphene, a semimetal, in many applications (e.g., electronics packaging). The size dependence of interfacial thermal conductance is first examined on a single-layer hexagonal boron nitride (h-BN)/hexane (C_6H_{14}) system. Then, a series of h-BN interfaces with organic molecules of different polarization groups as the matrixes are investigated. These include hexanamine ($C_6H_{13}NH_2$), hexanol ($C_6H_{13}OH$), and hexanoic acid ($C_5H_{11}COOH$). We note that our focus of this study is to understand how different functional groups in organic molecules influence thermal transport across their interfaces with h-BN. The selection of the above four materials largely eliminates the impact of the molecular chain length and backbone on the interfacial thermal transport, leaving the functional group the only factor that contributes to the change in interfacial thermal conductance. First, we define matrix regions based on the distances to the interface and calculate the nominal local thermal conductivities of these regions. It is interesting to find that the near-interface region tends to exhibit a higher density, which leads to a higher nominal local thermal conductivity. Compared to nonpolar matrix molecules, polar molecules are more strongly attracted to the BN layer and form a near-interface region of both higher density and higher nominal local thermal conductivity. Because of the higher near-interface density, more atoms join the energy exchange across the interface and lead to a higher interfacial thermal conductance. These results, although fundamental in nature, may have implications in the design of materials or nanostructures for different applications.

SIMULATION METHODS

Here, single-layer h-BN is used as the filler material, and four types of organic molecules, hexane (C_6H_{14}), hexanamine ($C_6H_{13}NH_2$), hexanol ($C_6H_{13}OH$), and hexanoic acid ($C_5H_{11}COOH$) are studied as matrixes. With similar carbon backbones and different end groups, the four types of organic molecules should have similar vibrational spectra,[27] but different polarizations. According to the group electronegativity of the functional groups in the four matrices (CH_3 2.17; NH_2 2.39; OH 2.85; COOH 3.09), the order of their polarity is $C_5H_{11}COOH$ > $C_6H_{13}OH$ > $C_6H_{13}NH_2$ > C_6H_{14} (Figure 1b).[28] Thus, the differences in the interfacial thermal conductance of these four h-BN−organic molecule systems may be mostly attributed to polarization.

The Tersoff potential[29] is used to describe the interaction among the h-BN atoms, and a modified universal force field[30] is used for the nonbonding interaction between h-BN and organic molecules. All 12-6 Lennard-Jones (L-J) coefficients associated with the h-BN atoms are listed in Table 1, and the cutoff is set to 10 Å. The charges of the B and N atoms in h-

Table 1. L-J Potential Parameters between the h-BN Atoms and the Rest of the Atoms

pair type	ε (kcal/mol)	σ (Å)
C−B	0.1374772708486750	3.53419521486273
O−B	0.1039230480000000	3.37784249000000
N−B	0.1114450530000000	3.44911438700000
H−B	0.0889943818451480	3.10433658336001
C−N	0.0851175657546667	3.34577013597604
O−B	0.0643428310000000	3.18941741100000
N−N	0.0690000000000000	3.66000000000000
H−N	0.0550999092558236	2.91591150447333

DOI: 10.1021/acsomega.8b02338
ACS Omega XXXX, XXX, XXX−XXX

BN are respectively 1.0 and −1.0, and the Hockney particle−particle particle−mesh[31] method is used here for the evaluation of coulomb energies and forces. The organic molecules are simulated using the polymer consistent force field.[32] All simulations are carried out using the large-scale atomic/molecular massively parallel simulator.[33] A timestep size of 0.25 fs is used for all simulations.

A typical structure is shown in Figure 1a. A single layer of h-BN is centered in the simulation domain with periodic boundary conditions (PBCs) in all three directions. The PBCs in the lateral directions model h-BN effectively infinite in size without edges. This is reasonable as the focus here is the interfaces between the basal plane of h-BN and the organic matrixes, and in reality, such interfaces are dominant in the composite. Each organic molecular system contains 200 molecules. The whole system is heated up to 600 K under an *NPT* (constant number of atoms, pressure, and temperature) ensemble to achieve a disordered amorphous phase and then cooled down to 300 K with an annealing speed of 12 K/ps. We note that the PBC in the direction perpendicular to the h-BN surface is necessary to ensure that the *NPT* optimization leads to the correct density of the organic liquid, which is important to the interfacial thermal transport.[34,35]

Nonequilibrium MD (NEMD) is used to calculate the interfacial thermal conductance. After the *NPT* relaxation at 300 K and 1 atm for 1.5−2 ns, the system is then simulated using an *NVE* (constant number of atoms, volume, and energy) ensemble with a heat source (320 K) and sink (280 K) imposed at the two ends of the system using Langevin thermostats (Figure 1a). A layer of atoms at each end of the simulation domain is fixed to prevent the heat transfer across the periodic boundaries, forcing all heat flux to cross the h-BN−organic molecule interface. The fixed atoms also prevent the translational drift of the whole system and thus help "lock" the position of the interface and extract the temperature profile. The relatively large temperature difference (40 K) is used to establish a measurable temperature gap across the interface. Except the fixed atoms, the rest of the system, including the thermostated regions, is simulated in the *NVE* ensemble for 10 ns for nominal local thermal conductivity and interfacial thermal conductance calculations at steady state. A typical temperature profile at the steady state is shown in Figure 1c. The heat flux (q) is calculated by averaging the energy input and output rates from the heat source and sink. The temperature jump (ΔT) across the interface is defined by the temperature difference between the organic molecules at the two sides of the h-BN layer. The interfacial thermal conductance (G) is then calculated as $G = q/\Delta T$. The nominal local thermal conductivity (κ) of the matrix is calculated as $\kappa = q/(\Delta T/L)$, where ΔT is the temperature difference between the two ends of the chosen region and L is the length of the chosen region. Figure 1d shows the temperature points used to calculate ΔT in regions A, B, and C; h-BN/hexane system is used here as an example. The whole system is divided into several equal-length bins, and the corresponding temperature is calculated for each bin. Then, the temperature points selected for each region are strictly based on the length of each region. The nominal local thermal conductivity is used to characterize the heat transfer capability of the region near the interface, which cannot be interpreted as the thermal conductivity of the organic liquid. We conduct two independent NEMD simulations for each system, and in each simulation, data at eight different time intervals (1 ns each) in the steady state are used for property calculations. Therefore, there are 16 data points averaged for each value of the interfacial thermal conductance. The error bars are the standard deviations of these data.

RESULTS AND DISCUSSION

The test on the size dependence of interfacial thermal conductance is first conducted to choose the appropriate system size for later simulations. The interfacial thermal conductance of systems with 200, 400, and 600 hexane molecules are respectively 88.01 ± 13.77, 104.21 ± 14.49, and 93.62 ± 32.43 MW/m^2 K. As all results are within their error bars, no size dependence is observed, and thus the system with the size of 200 organic molecules is selected, so as to save the simulation time but still produce justified calculations. We note that the thermal conductance for the h-BN/hexane interface calculated here is larger compared to that of the graphene/polyethylene interfaces (61 MW/m^2 K),[34] and this may be attributed to the stronger L-J interactions and additional electrostatic interactions across the h-BN/hexane interface.

Next, the nominal local thermal conductivities and densities of the hexane matrix with varying distances to the interface are calculated, and the results are shown in Figure 2. Three regions

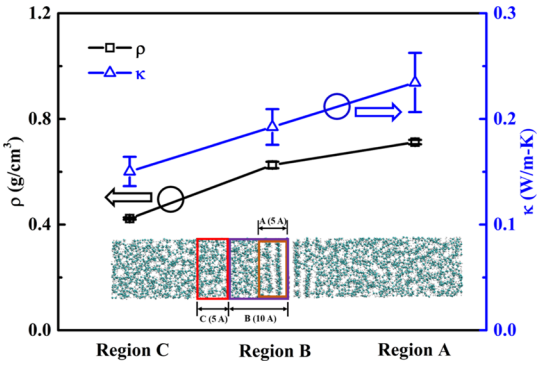

Figure 2. Nominal local thermal conductivities and densities of different regions in the h-BN/hexane system.

in the hexane matrix are chosen for exploration. Region A is the region within a distance of 5 Å next to the interface. Region B is the region within a distance of 10 Å next to the interface. Region C is the whole system, except for region B, region A, fixed region, heat source, and heat sink. Further, all the three regions contain only organic molecules. In Figure 2, it is found that when the hexane matrix gets closer to the h-BN interface, its nominal local thermal conductivity becomes larger. The higher nominal local thermal conductivity of the matrix near the interface can be attributed to the higher density of organic molecules,[36] as the corresponding density increases when approaching the interface.

Figure 3 shows the thermal conductivities and densities of different polar matrixes in region A, which is also called the near-interface region. According to the results in Figure 2, the region A shows the highest density and largest nominal local thermal conductivity. Therefore, the region A is being chosen for comparison among differently polarized matrixes, so as to offer the most representative results. It is interesting to find that when the organic matrix becomes more polarized, the organic molecules in the near-interface region have larger nominal local thermal conductivity, which could be explained by the corresponding higher density, as it is known that a

DOI: 10.1021/acsomega.8b02338
ACS Omega XXXX, XXX, XXX−XXX

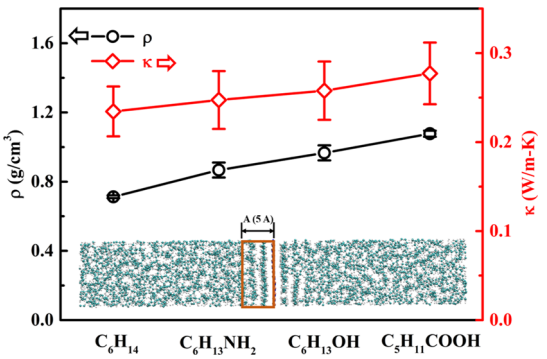

Figure 3. Nominal local thermal conductivities and densities of organic molecules at the near-interface region in the h-BN/hexane, h-BN/hexanamine, h-BN/hexanol, and h-BN/hexanoic acid systems.

higher density of a liquid can lead to a higher nominal local thermal conductivity because of the closer intermolecular distance.[26]

Finally, the thermal transport across the interface is being explored via calculating the interfacial thermal conductance of all the matrixes mentioned above. As Figure 4 shows, when the

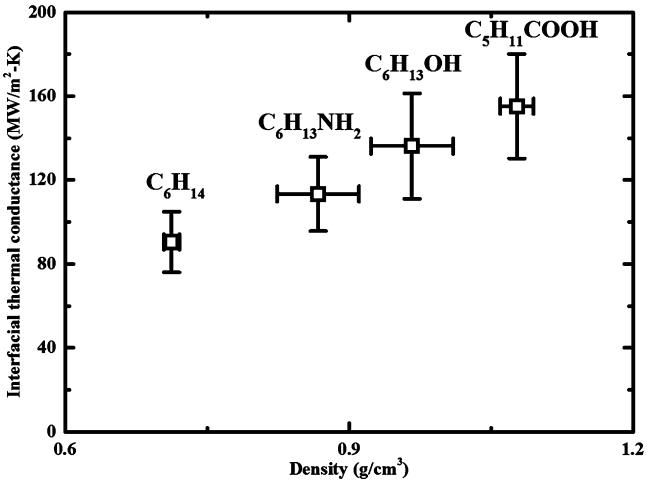

Figure 4. Interfacial thermal conductance of h-BN/hexane, h-BN/hexanamine, h-BN/hexanol, and h-BN/hexanoic acid as a function of the density of the organic molecules at the near-interface region.

matrix becomes more polarized, the interfacial thermal conductance becomes larger. Such an observation is well-correlated to the increasing trend of the local density of the matrix near the interface as the molecules become more polar. The more polar organic molecules are attracted by h-BN closer to the interface because of the stronger electrostatic interactions. Such a shorter interatomic distance can significantly enhance the heat flux contributed by the L-J interaction. In addition, the higher local density near the interface also allows more organic molecular atoms to have such close "contact" with the h-BN layer. In other words, it is the collaborative effect of the electrostatic and L-J interactions that leads to the observed increase in interfacial thermal conductance as a function of matrix molecular polarity.

CONCLUSIONS

In summary, we use the steady-state NEMD method to explore both the thermal transport across the interface and heat transfer within the matrix. Four types of organic molecules with different polarities are studied as the matrixes (hexane (C_6H_{14}), hexanamine ($C_6H_{13}NH_2$), hexanol ($C_6H_{13}OH$), and hexanoic acid ($C_5H_{11}COOH$). The nominal local thermal conductivities of the hexane matrix with varying distances to the interface are calculated to demonstrate the influence of the fillers on the matrix. It is found that the near-interface region will form a denser layer and exhibit a higher nominal local thermal conductivity, and such an effort is more pronounced for a more polar matrix. The higher density of the near-interface region in the more polar matrix also leads to a larger interfacial thermal conductance (hexane: 90.47 ± 14.49 MW/m^2 K, hexanamine: 113.38 ± 17.72 MW/m^2 K, hexanol: 136.16 ± 25.12 MW/m^2 K, and hexanoic acid: 155.17 ± 24.89 MW/m^2 K). These conclusions may be generalized to other organic molecules and polar filler materials. The results of this study may provide useful information for designing composite materials for heat transfer applications.

AUTHOR INFORMATION

Corresponding Authors

*E-mail: nuo@hust.edu.cn (N.Y.).
*E-mail: tluo@nd.edu (T.L.).

ORCID

Ruimin Ma: 0000-0003-1527-9289
Nuo Yang: 0000-0003-0973-1718
Tengfei Luo: 0000-0003-3940-8786

Author Contributions

‖R.M. and X.W. contributed equally to this work.

Notes

The authors declare no competing financial interest.

ACKNOWLEDGMENTS

N.Y. was sponsored by National Natural Science Foundation of China (no. 51576076 and no. 51711540031) and Hubei Provincial Natural Science Foundation of China (no. 2017CFA046). T.L. would also like to thank the National Science Foundation (1706039) for the financial support. This computation was supported in part by the University of Notre Dame, Center for Researching Computing, and NSF through XSEDE resources provided by SDSC Comet, TACC Stampede, National Supercomputing Center in Tianjin (NSCC-TJ) and China Scientific Computing Grid (ScGrid).

REFERENCES

(1) Dean, C. R.; Young, A. F.; Meric, I.; Lee, C.; et al. Boron nitride substrates for high-quality graphene electronics. *Nat. Nanotechnol.* **2010**, *5*, 722−726.
(2) Nag, A.; Raidongia, K.; Hembram, K. P. S. S.; Datta, R.; et al. Graphene analogues of BN: novel synthesis and properties. *ACS Nano* **2010**, *4*, 1539−1544.
(3) Notton, G.; Cristofari, C.; Mattei, M.; Poggi, P. Modelling of a double-glass photovoltaic module using finite differences. *Appl. Therm. Eng.* **2005**, *25*, 2854−2877.
(4) Goli, P.; Legedza, S.; Dhar, A.; Salgado, R.; et al. Graphene-enhanced hybrid phase change materials for thermal management of Li-ion batteries. *J. Power Sources* **2014**, *248*, 37−43.
(5) Shahil, K. M. F.; Balandin, A. A. Graphene-multilayer graphene nanocomposites as highly efficient thermal interface materials. *Nano Lett.* **2012**, *12*, 861−867.
(6) Goli, P.; Legedza, S.; Dhar, A.; Salgado, R.; et al. Graphene-enhanced hybrid phase change materials for thermal management of Li-ion batteries. *J. Power Sources* **2013**, *248*, 37−43.

DOI: 10.1021/acsomega.8b02338
ACS Omega XXXX, XXX, XXX−XXX

(7) Goyal, V.; Balandin, A. A. Thermal Properties of the Hybrid Graphene-Metal Nano-Micro-Composites: Applications in Thermal Interface Materials. *Appl. Phys. Lett.* **2012**, *100*, 073113.
(8) Balandin, A. A. Thermal properties of graphene and nano-structured carbon materials. *Nat. Mater.* **2011**, *10*, 569−581.
(9) An, M.; Song, Q.; Yu, X.; Meng, H.; et al. Generalized Two-Temperature Model for Coupled Phonons in Nanosized Graphene. *Nano Lett.* **2017**, *17*, 5805−5810.
(10) Song, W.-L.; Wang, P.; Cao, L.; Anderson, A.; et al. Polymer/boron nitride nanocomposite materials for superior thermal transport performance. *Angew. Chem., Int. Ed.* **2012**, *51*, 6498−6501.
(11) Yu, J.; Huang, X.; Wu, C.; Wu, X.; et al. Interfacial modification of boron nitride nanoplatelets for epoxy composites with improved thermal properties. *Polymer* **2012**, *53*, 471−480.
(12) Xie, B.-H.; Huang, X.; Zhang, G.-J. High thermal conductive polyvinyl alcohol composites with hexagonal boron nitride micro-platelets as fillers. *Compos. Sci. Technol.* **2013**, *85*, 98−103.
(13) Zhou, W.; Qi, S.; An, Q.; Zhao, H.; et al. Thermal conductivity of boron nitride reinforced polyethylene composites. *Mater. Res. Bull.* **2007**, *42*, 1863−1873.
(14) Li, T.-L.; Hsu, S. L.-C. Enhanced thermal conductivity of polyimide films via a hybrid of micro-and nano-sized boron nitride. *J. Phys. Chem. B* **2010**, *114*, 6825−6829.
(15) Sato, K.; Horibe, H.; Shirai, T.; Hotta, Y.; et al. Thermally conductive composite films of hexagonal boron nitride and polyimide with affinity-enhanced interfaces. *J. Mater. Chem.* **2010**, *20*, 2749−2752.
(16) Cahill, D. G.; Ford, W. K.; Goodson, K. E.; Mahan, G. D. Nanoscale thermal transport. *J. Appl. Phys.* **2003**, *93*, 793−818.
(17) Luo, T.; Chen, G. Nanoscale heat transfer–from computation to experiment. *Phys. Chem. Chem. Phys.* **2013**, *15*, 3389−3412.
(18) Zhang, T.; Gans-Forrest, A. R.; Lee, E.; Zhang, X.; et al. Role of hydrogen bonds in thermal transport across hard/soft material interfaces. *ACS Appl. Mater. Interfaces* **2016**, *8*, 33326−33334.
(19) Wei, X.; Zhang, T.; Luo, T. Thermal Energy Transport across Hard−Soft Interfaces. *ACS Energy Lett.* **2017**, *2*, 2283−2292.
(20) Renteria, J.; Legedza, S.; Salgado, R.; Balandin, M. P.; et al. Magnetically-functionalized self-aligning graphene fillers for high-efficiency thermal management applications. *Mater. Des.* **2015**, *88*, 214−221.
(21) Walther, J. H.; Jaffe, R.; Halicioglu, T.; Koumoutsakos, P. Carbon Nanotubes in Water: Structural Characteristics and Energetics. *J. Phys. Chem. B* **2001**, *105*, 9980−9987.
(22) Jaffe, R. L.; Gonnet, P.; Werder, T.; Walther, J. H.; et al. Water−Carbon Interactions 2: Calibration of Potentials using Contact Angle Data for Different Interaction Models. *Mol. Simul.* **2004**, *30*, 205−216.
(23) Alexeev, D.; Chen, J.; Walther, J. H.; Giapis, K. P.; et al. Kapitza Resistance between Few-Layer Graphene and Water: Liquid Layering Effects. *Nano Lett.* **2015**, *15*, 5744−5749.
(24) Gao, J.; Luedtke, W. D.; Landman, U. Layering Transitions and Dynamics of Confined Liquid Films. *Phys. Rev. Lett.* **1997**, *79*, 705−708.
(25) Wei, X.; Zhang, T.; Luo, T. Chain conformation-dependent thermal conductivity of amorphous polymer blends: the impact of inter- and intra-chain interactions. *Phys. Chem. Chem. Phys.* **2016**, *18*, 32146−32154.
(26) Zhang, T.; Luo, T. Role of Chain Morphology and Stiffness in Thermal Conductivity of Amorphous Polymers. *J. Phys. Chem. B* **2016**, *120*, 803−812.
(27) Swartz, E. T.; Pohl, R. O. Thermal resistance at interfaces. *Appl. Phys. Lett.* **1987**, *51*, 2200−2202.
(28) Mullay, J. Calculation of group electronegativity. *J. Am. Chem. Soc.* **1985**, *107*, 7271−7275.
(29) Tersoff, J. New empirical approach for the structure and energy of covalent systems. *Phys. Rev. B: Condens. Matter Mater. Phys.* **1988**, *37*, 6991−7000.
(30) Rappé, A. K.; Casewit, C. J.; Colwell, K. S.; Goddard, W. A., III; et al. UFF, a full periodic table force field for molecular mechanics and molecular dynamics simulations. *J. Am. Chem. Soc.* **1992**, *114*, 10024−10035.
(31) Beckers, J. V. L.; Lowe, C. P.; De Leeuw, S. W. An iterative PPPM method for simulating Coulombic systems on distributed memory parallel computers. *Mol. Simulat.* **1998**, *20*, 369−383.
(32) Sun, H.; Mumby, S. J.; Maple, J. R.; Hagler, A. T. An ab initio CFF93 all-atom force field for polycarbonates. *J. Am. Chem. Soc.* **1994**, *116*, 2978−2987.
(33) Plimpton, S. Fast parallel algorithms for short-range molecular dynamics. *J. Comput. Phys.* **1995**, *117*, 1−19.
(34) Luo, T.; Lloyd, J. R. Enhancement of thermal energy transport across graphene/graphite and polymer interfaces: a molecular dynamics study. *Adv. Funct. Mater.* **2012**, *22*, 2495−2502.
(35) Hung, S.-W.; Kikugawa, G.; Shiomi, J. Mechanism of temperature dependent thermal transport across the interface between self-assembled monolayer and water. *J. Phys. Chem. C* **2016**, *120*, 26678−26685.
(36) Guo, Z.; Lee, D.; Liu, Y.; Sun, F.; et al. Tuning the thermal conductivity of solar cell polymers through side chain engineering. *Phys. Chem. Chem. Phys.* **2014**, *16*, 7764−7771.

DOI: 10.1021/acsomega.8b02338
ACS Omega XXXX, XXX, XXX−XXX